

Dynamic saturation of an intersublevel transition in self-organized InAs/In_xAl_{1-x}As quantum dotsE. Péronne,^{1,2,*} F. Fossard,³ F. H. Julien,³ J. Brault,⁴ M. Gendry,⁴ B. Salem,⁵ G. Bremond,⁵ and A. Alexandrou¹¹Laboratoire d'Optique et Biosciences, UMR CNRS 7645, INSERM U451, Ecole Polytechnique–Ecole Nationale Supérieure de Techniques Avancées, F-91128 Palaiseau, France²Laboratoire d'Optique Appliquée, UMR CNRS 7639, Ecole Nationale Supérieure de Techniques Avancées–Ecole Polytechnique, F-91761 Palaiseau, France³Institut d'Electronique Fondamentale, UMR CNRS 8622, Université Paris-Sud, F-91405 Orsay, France⁴Laboratoire d'Electronique, Optoélectronique et Microsystèmes, UMR CNRS 5512, Ecole Centrale de Lyon, F-69134 Ecully, France⁵Laboratoire de Physique de la Matière, UMR CNRS 5511, Institut National des Sciences Appliquées de Lyon, F-69621 Villeurbanne, France

(Received 10 February 2003; published 30 May 2003)

We have observed a dynamic saturation of an intersublevel transition in InAs/In_xAl_{1-x}As quantum dots related to the discrete nature of electron states using midinfrared femtosecond spectroscopy. This dynamic saturation is a consequence of the gradual filling of the discrete quantum-dot electron states due to the capture of electrons injected in the barrier. Our interpretation of the differential transmission experiments is confirmed by a comparison with a rate-equation model with the capture and intersublevel relaxation time as fit parameters yielding 10 ps and 1 ps, respectively. We discuss the mechanism responsible for these relaxation times.

DOI: 10.1103/PhysRevB.67.205329

PACS number(s): 78.47.+p, 73.21.La

Electron dynamics in quantum dots (QD) has been the subject of controversy for quite a number of years. Early predictions based on electrons weakly coupled to a bath of longitudinal-optical (LO) phonons predicted a drastic decrease of relaxation rates in quantum dots caused by the discrete nature of energy states, the so-called phonon-bottleneck effect.^{1,2} However, this relaxation slow down has eluded experimental observation.^{3–8} Different theoretical explanations were given for the short relaxation times observed: Carrier-carrier interaction^{9–11} and, in particular, electron-hole interaction has been proposed to be responsible for fast relaxation. Relaxation of electrons captured in the absence of holes was found to be much slower in II–VI (Ref. 5) and III–V (Ref. 7) QDs. Inoshita and Sakaki¹² proposed multiphonon relaxation pathways involving combinations of LO and longitudinal-acoustical (LA) phonons as efficient relaxation mechanisms for transition energies different from the LO-phonon energy by a few meV. Recently, a strong-coupling approach of the electron–LO-phonon interaction leading to the formation of polarons was introduced.^{13–15} Relaxation times on the order of several tens of picoseconds for large detunings from the LO-phonon energies were measured in InAs/GaAs QD's and explained in terms of polaron relaxation driven by the finite lifetime of the optical phonons.⁸

The intersublevel relaxation time also determines the saturation dynamics of intersublevel transitions. Saturation of intersublevel transitions has been observed both in quantum wells¹⁶ and in quantum dots³ by pumping electrons in *n*-doped samples from the ground state to the excited state using a midinfrared pump and was used to deduce the intersublevel relaxation time. Indeed, as the pump excitation density is increased, the population of the excited state becomes equal to that of the ground state and the intersublevel absorption goes to zero.

We here report the observation of a *dynamic* saturation taking place in undoped InAs/In_xAl_{1-x}As QD's as a function of time for a constant pump excitation density that injects electrons in the barrier. As electrons are captured, they pro-

gressively fill the ground state, giving rise to an increasing intersublevel absorption measured with a midinfrared probe that reaches a maximum when the ground state is filled. As further electrons are captured occupying the excited state of the transition, the intersublevel absorption decreases. The observability of this dynamic saturation is related to the discrete nature of quantum-dot states. Measurements as a function of pump intensity and comparison with a rate-equation model confirm this interpretation related to the discrete nature of the quantum-dot states and yield the capture and intersublevel relaxation time.

The InAs/In_xAl_{1-x}As QD's were grown at 525 °C using solid-source molecular beam epitaxy on a semi-insulating InP(001) substrate. A 0.4-μm-thick lattice-matched In_{0.52}Al_{0.48}As buffer layer was first grown in anion-stabilized conditions with a beam equivalent pressure (BEP) of arsenic of about 7 × 10⁻⁶ Torr. The last 0.3 nm were grown in cation-stabilized conditions with an arsenic BEP of 7 × 10⁻⁷ Torr, producing island precursors from InAlAs, as indicated by the reflection high-energy electron diffraction pattern (RHEED), before the InAs deposition. Then, 3.5 monolayers (ML) of InAs were grown in anion-stabilized conditions with an arsenic BEP of 5 × 10⁻⁶ Torr before capping with a 0.3-μm-thick InAlAs layer. In the InAs/In_xAl_{1-x}As system, for InAs thicknesses above the two- to three-dimensional growth mode transition (2.5 ML), wires or dots can be obtained depending on the growth conditions and, in particular, on the InAlAs surface preparation.^{17,18} The growth conditions chosen here are optimized for quantum-dot growth.

Figure 1(a) shows a typical atomic-force microscopy (AFM) image of a quantum-dot sample grown in the same conditions as the sample studied here. The mean height, width, and length of the dots, measured from the AFM image, are 5.0 ± 1.0 nm, 40 ± 10 nm, and 60 ± 10 nm, respectively. Note that AFM images usually overestimate the lateral dimensions by a factor of about 1.2 and underestimate the height.

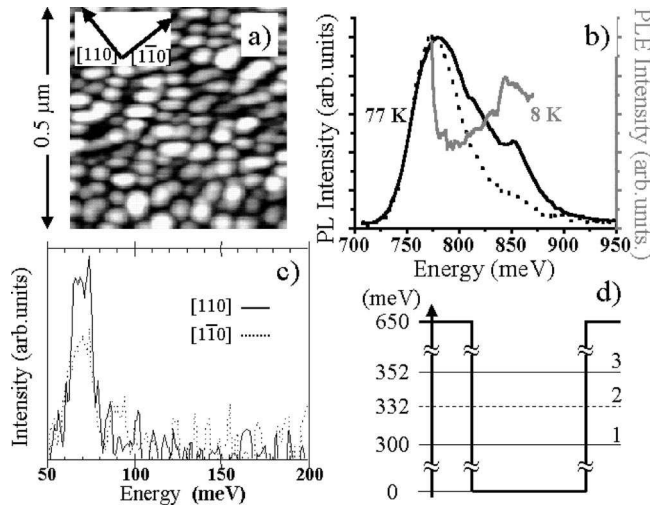


FIG. 1. (a) AFM image of a typical noncapped QD plane. (b) Photoluminescence (PL) of the sample at 77 K at low excitation (200 W cm^{-2} , dotted curve) and high excitation (4 kW cm^{-2} , solid curve) and PLE spectrum at 8 K (gray curve). (c) Photoinduced infrared absorption (PIA) of the sample for two different polarizations. (d) Calculated energy diagram (see text).

The photoluminescence spectrum at 77 K of our sample is shown in Fig. 1(b). As the excitation power increases, a peak appears at about 70 meV above the main peak due to photoluminescence from an excited-state transition of the QDs.¹⁹ The existence of this excited-state transition is confirmed by photoluminescence excitation (PLE) experiments at 8 K which show an absorption peak around 70 meV above the ground-state transition [Fig. 1(b); the photoluminescence (PL) spectrum at 8 K (not shown) peaks at 770 meV].

We measured the midinfrared photoinduced absorption (PIA) at normal incidence for $[110]$ and $[1\bar{1}0]$ polarizations by irradiating the sample with a cw argon-ion laser. The spectra show a strong in-plane polarized absorption starting at 80 meV [Fig. 1(c)]. The decrease and disappearance of the signal at 50 meV are due to the detector cutoff. When the spectra of Fig. 1(c) are divided by the measured transmitted intensity in the absence of visible excitation, an absorption signal continuously increasing up to 50 meV is obtained, which means that the absorption peak probably lies below 50 meV. The comparison with effective-mass calculations discussed below leads us to attribute this absorption to an intersublevel (ISL) transition in the conduction band between the ground state and the first excited state due to the smaller lateral size of the dots. The excited electron state is most probably the same as that involved in the excited-state transition observed in PL and PLE spectra. This means that another excited state should exist at lower energy (below the range of sensitivity of our detector) due to the larger lateral size of the dots. The higher absorption signal along $[110]$ is related to a preferential orientation of the shorter dot axis. The observations of ISL absorption for both $[110]$ and $[1\bar{1}0]$ polarizations and of an excited-state transition in PL and PLE²⁰ confirm the dotlike nature of the self-organized nanostructures seen in the AFM image.

We performed three-dimensional (3D) effective-mass cal-

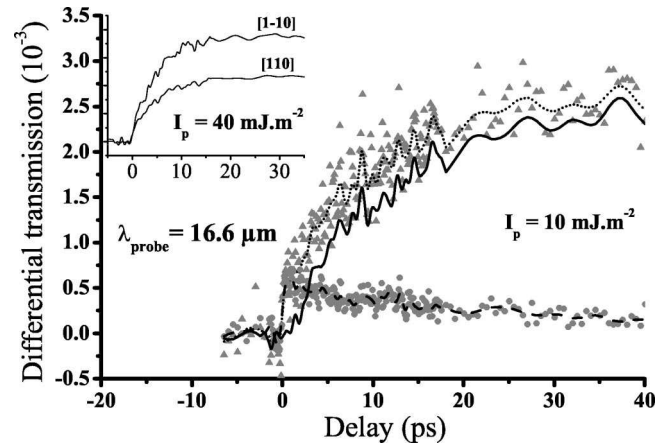


FIG. 2. Differential transmission signal measured for a probe polarized along $[110]$ (triangles) and free-carrier absorption (FCA) signal (circles; see text). Smoothed data obtained by averaging over five points are shown as dotted and dashed lines, respectively. The solid line was obtained by subtracting the FCA signal from the measured differential transmission and is due to the intersublevel (ISL) quantum-dot absorption. The individual experimental points are not shown for clarity. The inset shows the DT signal for two different probe polarizations $[110]$ and $[1\bar{1}0]$.

culations of the ISL transition energies²¹ using a lens-shaped dot with dimensions inferred from the AFM data after application of the above-cited 1.2 correction factor and a 0.6–0.9-nm-thick wetting layer observed in transmission electron microscopy images of samples with the same deposited thickness of InAs. The calculated energy differences between the first excited and the ground electron state due to the short- (long-) axis confinement yield 52 (32) meV, respectively, in quite good agreement with the PL, PLE, and PIA data. An approximate energy diagram is sketched in Fig. 1(d).²²

In order to probe the ISL transition dynamics, we performed differential transmission (DT) experiments using a 200-kHz-rate amplified Ti:sapphire laser delivering 130-fs pulses centered at 800 nm. The output beam is split in two: one beam generates a white-light continuum and seeds an optical parametric amplifier (OPA) and the other one pumps the OPA. The remaining pump intensity after the OPA is used to excite carriers in the InAlAs barriers. Difference frequency mixing from the output of the near-infrared OPA generates midinfrared pulses in an AgGaSe₂ crystal. The midinfrared pulses are tuned to $\lambda = 16.6 \mu\text{m}$, to the high-energy side of the ISL absorption corresponding to the smaller-sized dots, thus allowing to exclusively probe the electron dynamics. The experiments were performed at room temperature using lock-in detection.

The DT (Fig. 2) shows an initial fast rise time independent of probe polarization and a slower rising component with amplitudes showing the same polarization ratio as in the PIA experiments (see inset). As in our previous work on quantum-wire samples in the same material system,²³ we ascribe the initial fast rise time to free-carrier absorption (FCA) in the barrier layers of the sample following the generation of electron-hole pairs by the visible pump. This attribution is confirmed by comparing the DT signal to the one obtained

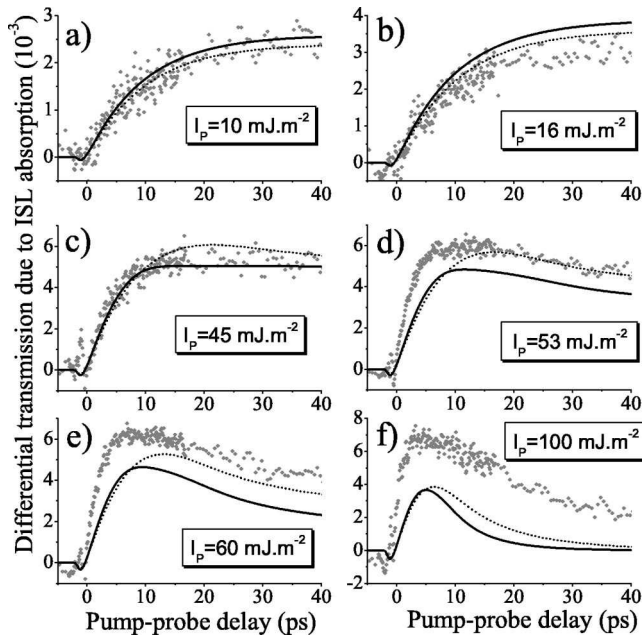


FIG. 3. Differential transmission for several pump energy densities. The fits of the data are shown for a three-level rate equation model (dotted curves) and for a four-level rate equation model (solid curves) (see text).

for FCA absorption only, at equal pump intensity in a quantum-wire sample with the same thickness of capping layer, where no intersublevel absorption is observed for a $[1\bar{1}0]$ probe polarization.²³ Since this FCA signal was measured at $\lambda = 13 \mu\text{m}$ we have extrapolated its amplitude at $\lambda = 16.6 \mu\text{m}$ using the theoretical λ^3 dependence of the FCA.²⁴ The decay of the FCA signal is due to electron-hole recombination. Because the FCA instantaneously follows the pump profile, it provides an accurate way to determine the full width at half maximum (FWHM) of the pump-probe convolution ($\Delta t = 375$ fs) and the zero delay (t_0). The slower rising component of the DT is due to the ISL absorption and is proportional to the population difference between the excited state and the ground state of the transition. We isolate the intersublevel contribution to the signal by subtracting the FCA signal. The result is shown as a solid line in Fig. 2 and shows a characteristic delay with respect to the zero pump-probe delay indicative of a non-negligible intersublevel relaxation time.²³

We then varied the excitation density in order to measure the effect of occupation on the relaxation time. The ISL absorption obtained from the differential transmission after subtracting the FCA contribution for various pump intensities (I_p) is shown in Fig. 3. The FCA contribution was removed as following: When the steplike structure due to FCA was clearly visible in the DT spectra (a–c), we used the amplitude of the step and the decay behavior of the FCA signal measured at $\lambda = 13 \mu\text{m}$ at equal pump intensity in a sample with the same thickness of capping layer. In the case of the three highest pump intensities (d–f), where the steplike rise in the DT signal was not clearly identifiable, we extrapolated the amplitude from the $\lambda = 13 \mu\text{m}$ signal using the theoretical λ^3 dependence of the FCA.²⁴ At low injected

carrier densities, the ISL absorption increases as a function of pump-probe delay, reaches a maximum, and then remains constant at later delays. The decay of this long-lasting signal is related to the emptying of the electron ground state due to radiative recombination. Furthermore, the maximum reached is proportional to the pump intensity [Fig. 3(a,b)]. At higher electron densities, the ISL absorption signal reaches a maximum earlier and then decreases as a function of pump-probe delay. Moreover, the maximum of the ISL signal is no longer proportional to the pump excitation density but shows a saturation behavior.

The results at higher electron densities can be explained as manifestations of a dynamic saturation of the ISL transition. As electrons are gradually captured from the barrier and relax to the electron ground state, the occupation factor of the ground state tends to 2. For longer pump-probe delay times, any existing intermediate electron levels between the two electron levels involved in the probed ISL transition are filled up and then the excited level of the transition starts being occupied. At this point, the ISL absorption signal should decrease as observed in the experiment. It should be stressed that this dynamic saturation is due to the discrete nature of the quantum-dot electron states and was not observed in quantum-wire samples at similar pump intensities.²³

In order to confirm this interpretation, we used a rate-equation model taking into account the saturation effect. In a first approximation, we consider in our model only three levels: one for the barrier where electrons are injected and the two levels of the ISL transition we are probing. The generation rate is assumed to be a Gaussian centered at t_0 with a width Δt . The fit parameters are the capture time from the barrier to the excited state (τ_{c3}), the capture time from the barrier directly to the ground state (τ_{c1}), and the ISL relaxation time between the two states of the transition (τ_{31}). The same values were used for all pump intensities. Introducing a density dependence of the capture and relaxation times may slightly improve the agreement with experiment but we preferred not to add further fit parameters. In agreement with theoretical predictions,⁹ the fit procedure yields a capture time τ_{c1} much longer than the capture time τ_{c3} , a capture time $\tau_{c3} = 10 \pm 1$ ps, and an ISL relaxation time $\tau_{31} = 1 \pm 0.2$ ps (see dotted lines in Fig. 3). A total concentration of 0.6 electrons per dot was used for Fig. 3(a) and was linearly scaled with pump intensity. An estimate of the electron density can be obtained from the absorption coefficient of In-AlAs assuming a capture into the QD's from a thickness of 50 nm on both sides of the quantum-dot plane, which gives 0.5 electrons/dot for a pump excitation density of 10 mJ m^{-2} . The uncertainty related to the above assumption justifies the use of a somewhat higher electron density in the calculation. For the highest excitation densities, although the calculation qualitatively agrees with the experimental data, its amplitude is weaker. This is probably due to difficulties in correctly subtracting the FCA signal in a regime where it dominates the differential transmission.

Given the existence of a large-axis confinement in these dots, an intermediate excited electron level most probably exists between the ground state and the excited state in-

volved in the ISL transition we are probing. Therefore, a four-level system is more adequate for the description of the data. The results obtained in this case using an electron density of 0.9 electrons/dot for the lowest pump intensity are shown as solid lines in Fig. 3. The same values were used for τ_{c3} and τ_{31} . Here, however, τ_{31} includes not only the ISL relaxation directly from level 3 to 1, but also relaxation processes from level 3 to 2 and subsequently from 2 to 1 which are probably more efficient since they involve smaller transition energies closer to the LO-phonon energy (30 meV in InAs). Good agreement with the experiment is obtained, thus confirming the interpretation of the experimental behavior in terms of dynamic saturation of the intersublevel transition.

The capture time extracted here is longer than the one measured in the InAs/In_xAl_{1-x}As quantum-wire case.²³ However, the present sample consists of only one quantum-dot plane, which means that the contribution of transport processes to the capture time cannot be excluded. Thus, the 10-ps capture time should be viewed as an upper limit of the quantum capture time.

Although the ISL relaxation time is longer than that measured in quantum wires,²³ it is still much shorter than what would be expected for a 75-meV transition. Due to the presence of an intermediate electron level, however, relaxation can take place via two ISL transition steps with energies

close to the LO-phonon energy. Emission processes of combinations of two phonons (LO + LA or LO-LA) have been calculated to be responsible for very short relaxation times (on the order of 1 ps) when the transition energy is close to the LO-phonon energy.¹² The polaronic picture of strong coupling between electrons and phonons can also give relaxation values compatible with the 1-ps relaxation time deduced here. Both these processes are very sensitive to the precise energy of the intermediate electron level. Since this is not known, a more accurate comparison with theory is not possible. Furthermore, the contribution of electron-hole scattering cannot be excluded because geminate capture⁷ probably dominates even at the lowest excitation levels used here.

In conclusion, we have observed a dynamic saturation of an intersublevel transition between zero-dimensional (0D) electron levels in self-organized InAs/In_xAl_{1-x}As QDs using differential transmission in the midinfrared region. The experimental behavior can be well reproduced using a rate-equation model that takes into account the gradual filling of the electron levels as electrons are captured from the barrier states. In addition, we have been able to determine an upper limit for the quantum capture time of 10 ps and to extract an intersublevel relaxation time of 1 ps.

We are grateful to Ana Helman for help with the PIA experiments.

*Present address: Department of Chemistry, University of Aarhus, DK-8000 Aarhus C., Denmark.

¹U. Bockelmann and G. Bastard, *Phys. Rev. B* **42**, 8947 (1990).

²H. Benisty, C. M. Sotomayor-Torrès, and C. Weisbuch, *Phys. Rev. B* **44**, 10 945 (1991).

³S. Sauvage, P. Boucaud, F. Glotin, R. Prazeres, J. M. Ortega, A. Lemapitre, J. M. Gérard, and V. Thierry-Mieg, *Appl. Phys. Lett.* **73**, 3818 (1998).

⁴P. Guyot-Sionnest, M. Shim, C. Matranga, and M. Hines, *Phys. Rev. B* **60**, R2181 (1999).

⁵V. I. Klimov, A. A. Mikhailovsky, D. W. McBranch, C. A. Leatherdale, and M. G. Bawendi, *Phys. Rev. B* **61**, 13 349 (2000).

⁶J. Feldmann, S. T. Cundiff, M. Arzberger, G. Böhm, and G. Abstreiter, *J. Appl. Phys.* **89**, 1180 (2001).

⁷J. Urayama, T. B. Norris, J. Singh, and P. Bhattacharya, *Phys. Rev. Lett.* **86**, 4930 (2001).

⁸S. Sauvage, P. Boucaud, R. P. S. M. Lobo, F. Bras, G. Fishman, R. Prazeres, F. Glotin, J. M. Ortega, and J. M. Gérard, *Phys. Rev. Lett.* **88**, 177402 (2002).

⁹U. Bockelmann and T. Egeler, *Phys. Rev. B* **46**, 15 574 (1992).

¹⁰A. V. Uskov, J. McInerney, F. Adler, H. Schweizer, and M. H. Pilkuhn, *Appl. Phys. Lett.* **72**, 58 (1998).

¹¹R. Ferreira and G. Bastard, *Appl. Phys. Lett.* **74**, 2818 (1999).

¹²T. Inoshita and H. Sakaki, *Phys. Rev. B* **46**, 7260 (1992).

¹³T. Inoshita and H. Sakaki, *Phys. Rev. B* **56**, R4355 (1997).

¹⁴X.-Q. Li, H. Nakayama, and Y. Arakawa, *Phys. Rev. B* **59**, 5069 (1999).

¹⁵O. Verzelen, R. Ferreira, and G. Bastard, *Phys. Rev. B* **62**, R4809 (2000); *Phys. Rev. Lett.* **88**, 146803 (2002).

¹⁶F. H. Julien, J.-M. Lourtioz, N. Herschkorn, D. Delacourt, J.-P.

Pocholle, M. Papuchon, R. Planel, and G. Le Roux, *Appl. Phys. Lett.* **53**, 116 (1988); **62**, 2289 (1993).

¹⁷J. Brault, M. Gendry, G. Grenet, G. Hollinger, J. Olivres, B. Salem, T. Benyattou, and G. Bremond, *J. Appl. Phys.* **92**, 506 (2002).

¹⁸F. Fossard, F. H. Julien, E. Péronne, A. Alexandrou, J. Brault, and M. Gendry, *Infrared Phys. Technol.* **42**, 443 (2001).

¹⁹A weaker shoulder is observed at about 40 meV above the main peak, which may be due to an excited-state transition related to the large-axis confinement of the dots.

²⁰Saturation of the ground-state transition and excited-state transitions are not observed in quantum wires under the same excitation conditions.

²¹The Ben Daniel-Duke Hamiltonian was discretized and diagonalized using the implicitly restarted Arnoldi method. The mass values used were 0.084, 0.68, and 0.084 for electrons, heavy holes, and light holes, respectively, in In_xAl_{1-x}As and 0.027, 0.51, and 0.027 for electrons, heavy holes, and light holes, respectively, in InAs. The conduction (valence) band discontinuity was 650 (355) meV.

²²The confinement energy of the first excited electron level is obtained from the interband transition energy measured in the PL experiment and from the energy band gap of InAs at 77 K (420 meV) assuming a ratio of 6 between the electron and hole confinement energy.

²³E. Péronne, T. Polack, J.-F. Lampin, F. Fossard, F. Julien, J. Brault, M. Gendry, O. Marty, and A. Alexandrou, *Phys. Rev. B* **63**, 081307 (2001).

²⁴C. Seeger *Semiconductor Physics*, (Springer-Verlag, Berlin, 1986).